Journal of Solid Mechanics Vol. 12, No. 1 (2020) pp. 175-188
DOI: 10.22034/jsm.2019.1864818.1412

The Dynamic and Vibration Response of Composite Cylindrical Shell Under Thermal Shock and Mild Heat Field

S.A. Mousavi, M. Rahmani, , M. Kaffash Mirzarahimi, S. Mahjoob Moghadas *

Mechanical Engineering Faculty, Imam Hossein University, Thehran, Iran

Received 5 December 2019; accepted 2 February 2020

ABSTRACT

In this article, the vibration and dynamic response of an orthotropic composite cylindrical shell under thermal shock loading and thermal field have been investigated. The problem is that the shell is initially located at a first temperature, and some tension caused by a mild heat field is created, then the surface temperature of the cylinder suddenly increases. The partial derivative equations of motion are in the form of couplings with the heat equations. First, the equations of motion are derived by the Hamilton principle; here first-order shear theory and considering strain-shift relations of Sanders are used. Then, the equation system including the equations of motion and energy equations by the Runge–Kutta fourth-order method are solved. In this study, the effects of length, temperature, thickness and radius parameters on natural frequencies and intermediate layer displacement are investigated. The results show that the increase in external temperature decreases the natural frequency and increases the displacement of the system. In addition, the results of radial transitions were evaluated with previous studies and it was found that it is in good agreement with the results of previous papers.

Keywords: Thermal shock; Composite; Thermal field; Vibration.

1 INTRODUCTION

COMPOSITE materials have identified their position in engineering and are now used at various points as common materials, especially for structural purposes. Today, in the military industry, airplane, automotive, construction of sporting and entertainment products, electronics, mechanical and medical materials, composite materials are used. One of the most important structures used in various industries is the thin-walled cylindrical shells used in various applications The use of thermoelastic behavior of cylindrical shells subject to extreme temperature changes is very important in the design of advanced engineering structures. However, both in metal structures and in composite structures, the temperature changes both during production and when used are very common. Changes in temperature make two important effects. First, the amount of material is expanded when the

*Corresponding author. Tel.: +98 09120364932.
E-mail address: Smahjoubmoghadas@ihu.ac.ir (S. Mahjoob Moghadas).

temperature rises and contracted when cools. This expansion and contraction are usually proportional to the temperature variation. The thermal expansion coefficient α is a constant correlation between thermal strain and temperature variation relative to a reference temperature. In which there is no strain or thermal stress. The second effect relates to the stiffness and strength of the material; many materials become softer, more flexible and weaker when heated. Unwanted vibrations in systems result in poor performance, system life, or major failures and system disruptions, resulting in huge economic losses. Therefore, initial studies to control the vibrations of any system can prevent the occurrence of vibration problems when using the system. In this study, the dynamic response and the frequency response of composite cylindrical shells under thermal shock and a mild initial thermal field are Studied.
One of the first studies in this field is the McQuillen, E.J. and Brull [1] paper, by numerical studies They checked the thermoelastic coupling of a thin cylindrical shell by using the traditional Gallerican method. In that study, they considered a nonlinear distribution of temperature in the shell thickness, and found that the difference between the coupling and non-coupling was about 1%. Fundamental monograph about coupled thermoelasticity was published by Biot [2]. The thermal problems of the theory of plates and shells have been considered in the series of monographs [3–8]. In addition, we would like to mention also the following important works devoted to the subject of the paper. Thermal stress solution of conical shells (semi-coupled) was first considered by Huth [9,10]. The coupled thermoelasticity of shells of revolution was studied by Eslami et al. [11–13], based on second-order shell theory, and the governing equations including normal stress and strain as well as the transverse shear and rotary inertia were considered. Coupled dynamic thermoelastic equations of cylindrical thin shells were solved by Hakimelahi and Soltani [14] who used the numerical Galerkin method. They assumed variable mechanical and thermal shocks along the cylindrical shell with axial displacement and parabolic temperature distribution through thickness. Dynamic equilibrium equations of conical shells were obtained by Eslami and Moosavi [15] using a general linear theory which includes normal and lateral shear stresses and assuming dependency of strain field on temperature. Thus, semicoupled dynamic equations of conical shells were derived and solved by using the Galerkin finite element method. Tarn[16] examined the exact solution of thermal and thermal loads on a FGM cylinder. In his research, he considered the Yang model as a function of radius. In this study, a precise solution is presented for temperature distribution, thermoelastic deformation and stress field for a non-homogeneous thick cylinder. Alibeigloo [17] studied the thermoesthetic problem of static deformations in piezoelectric coated cylindrical shells. He used Navier's and state space methods to solve ordinary differential equations and the governing equations. R. Ansari,and J. Torabi [18] Free vibrations of cylindrical shells made of functional reinforced composites with carbon nanotubes under thermal loading and enclosed by elastic substrates have been investigated. They have affected the various parameters such as thermal loading, different boundary conditions, elastic bedding and geometric conditions Different on the natural frequency of the structure. Alibeigloo [19] studied the Elasticity solution of functionally graded carbon nanotube-reinforced. Y. Kiani and M. Eslami [20] Based on the uncoupled thermoelasticity assumptions, axisymmetric thermally induced vibrations of a circular plate with the arbitrary type of time-dependent boundary conditions made of FGM are analyzed. S.E. Ghiasian et al. [21] studied geometrically nonlinear thermally induced vibrations of functionally graded material beams and solved via a hybrid iterative central finite difference method and Crank-Nicolson method. S. M. Alipour et al. [22] investigated thermally induced vibrations of functionally graded material rectangular plates and solved the equation by means of the GDQ accompanied by the successive Runge–Kutta algorithm in the time domain. A. Keibolahi et al. [23] analyzed large amplitude thermally induced vibrations of a shallow curved beam that is made from an isotropic homogeneous material. H. R. Esmaeili et al. [24] investigated Large amplitude thermally caused vibrations of cylindrical shells made of a through-the-thickness FGM. All of the thermo-mechanical properties of the FGM shell are considered to be functions of temperature and thickness coordinate. A. Keibolahi et al. [25] studied the dynamic buckling of a shallow arch subjected to a transient type of thermal loading by following the Budiansky–Hutchinson criterion. M. Javani et al. [26] analyzed nonlinear vibrations of the FGM shallow arches subjected to different sudden thermal loads Based on the uncoupled thermoelasticity assumptions. The heat equations solved numerically by a hybrid iterative GDQ method and Crank-Nicolson time marching scheme. M. Javani et al. [27] investigated large amplitude thermally induced vibrations of an annular FGM plate subjected to rapid surface heating.

2 PROBLEM FORMULATION

Consider a thin cylindrical shell of thickness h and an average radius R in the coordinates (x, Θ, z), as shown in Fig. 1, which z is measured from the midpoint of the cylinder, it is assumed that this The shell is on a uniform thermal field, with which it reaches the thermal equilibrium and suddenly it enters a thermal shock (this shock can be a

sudden increase in temperature at either one of the internal or external surfaces, or both), The shell is isolated on its edges and the boundary conditions are considered to be clamped.

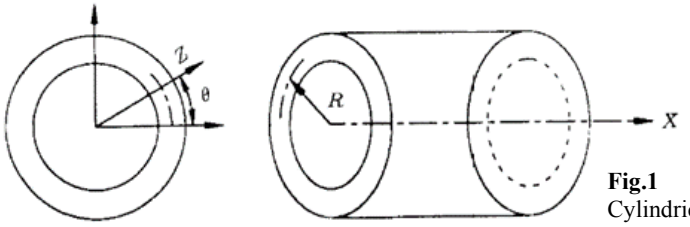

Fig.1
Cylindrical shell coordinates.

In order to obtain the governing equations, a relatively thin cylindrical shell is assumed to be hypothesized. The displacement components are based on the first order approximation of the shells as follows [28]:

$$U\left(x,\theta,z\right)=u_0(x,\theta)+z\psi_x(x,\theta,0) \tag{1}$$

$$V\left(x,\theta,z\right)=v_0\left(x,\theta\right)+z\psi_\theta(x,\theta,0) \tag{2}$$

$$W\left(x,\theta,z\right)=w_0\left(x,\theta\right) \tag{3}$$

In these relations, u_0, v_0 and w_0 represent the components of displacement vector of the point on the middle of the crust, and ψ_x and ψ_θ represent the rotation of the tangents of the middle surface along the x and Θ axes, respectively. Therefore, in the hypothesized theory is just the normal strain $\varepsilon_z = 0$, the components of other normal and shear strains at each point of the cylindrical thickness are obtained as follows [29]:

$$\begin{aligned}
&\varepsilon_x=\frac{\partial u}{\partial x} \qquad \varepsilon_\theta=\frac{1}{R}\left(\frac{\partial v}{\partial x}+w\right) \qquad \varepsilon_{x\theta}=\frac{\partial v}{\partial x}+\frac{1}{R}\frac{\partial U}{\partial \theta} \qquad \varepsilon_{x\theta}=\frac{1}{R}\frac{\partial w}{\partial x}-\frac{v}{R}+\psi_\theta \qquad \varepsilon_{xz}=\frac{\partial w}{\partial x}+\psi_x \\
&k_x=\frac{\partial \psi_x}{\partial x} \qquad k_\theta=\frac{1}{R}\frac{\partial \psi_\theta}{\partial \theta} \qquad k_{x\theta}=\frac{1}{R}\frac{\partial \psi_x}{\partial \theta}+\frac{\partial \psi_\theta}{\partial x}+\frac{1}{2}\frac{1}{R}\left(\frac{\partial v}{\partial x}+\frac{1}{R}\frac{\partial u}{\partial \theta}\right)
\end{aligned} \tag{4}$$

According to Hooke's law, stresses are obtained according to strain components as follows [28]:

$$\begin{Bmatrix}\sigma_x\\ \sigma_\theta\\ \sigma_z\\ \tau_{\theta z}\\ \tau_{xz}\\ \tau_{x\theta}\end{Bmatrix}=\begin{bmatrix}\bar{Q}_{11} & \bar{Q}_{12} & \bar{Q}_{13} & \bar{Q}_{14} & 0 & 0\\ \bar{Q}_{21} & \bar{Q}_{22} & \bar{Q}_{23} & \bar{Q}_{24} & 0 & 0\\ \bar{Q}_{31} & \bar{Q}_{32} & \bar{Q}_{33} & \bar{Q}_{34} & 0 & 0\\ \bar{Q}_{41} & \bar{Q}_{42} & \bar{Q}_{43} & \bar{Q}_{44} & 0 & 0\\ 0 & 0 & 0 & 0 & \bar{Q}_{55} & \bar{Q}_{56}\\ 0 & 0 & 0 & 0 & \bar{Q}_{65} & \bar{Q}_{66}\end{bmatrix}\times\left(\begin{bmatrix}\varepsilon_x\\ \varepsilon_\theta\\ \varepsilon_z\\ \gamma_{\theta z}\\ \gamma_{xz}\\ \gamma_{x\theta}\end{bmatrix}-\begin{bmatrix}\alpha_{11}\\ \alpha_{22}\\ \alpha_{33}\\ 0\\ 0\\ 0\end{bmatrix}\Delta T\right) \tag{5}$$

Note that the coefficients of thermal expansion affect the longitudinal strain and have no effect on the shear strain. In addition, in the present problem, each layer is transversally isotropic (in directions 2 and 3, the properties are similar), and we have $v_{12} = v_{13}$, $G_{12} = G_{13}$, $E_{22} = E_{33}$, and the simplifications for Q_{ij} coefficients are expressed as follows [30]:

$$Q_{11}=\frac{E_1}{1-v_{12}v_{21}} \qquad Q_{12}=Q_{21}=\frac{v_{12}E_2}{1-v_{12}v_{21}} \qquad Q_{22}=\frac{E_2}{1-v_{12}v_{21}} \qquad Q_{66}=G_{12} \tag{6}$$

For a single layer of composite:

$$\begin{Bmatrix}\sigma_x\\ \sigma_\theta\\ \tau_{x\theta}\end{Bmatrix}=\begin{bmatrix}\bar{Q}_{11} & \bar{Q}_{12} & 0\\ \bar{Q}_{21} & \bar{Q}_{21} & 0\\ 0 & 0 & \bar{Q}_{66}\end{bmatrix}\begin{Bmatrix}\varepsilon_x-\alpha_{11}\Delta T\\ \varepsilon_\theta-\alpha_{11}\Delta T\\ \gamma_{x\theta}\end{Bmatrix} \tag{7}$$

According to the stresses presented in relation 8, forces and moments will be as follows [30]:

$$(N_i, M_i)=\int_{-h/2}^{h/2}\sigma_i(1,z)dz \tag{8}$$

$$Q_i=\int_{-h/2}^{h/2}\sigma_i dz \tag{9}$$

$$\begin{bmatrix}N_x\\ N_\theta\\ N_{x\theta}\\ M_x\\ M_\theta\\ M_{x\theta}\\ Q_x\\ Q_\theta\end{bmatrix}=\begin{bmatrix}A_{11} & A_{12} & 0 & B_{11} & B_{12} & 0 & 0 & 0\\ A_{12} & A_{22} & 0 & B_{12} & B_{22} & 0 & 0 & 0\\ 0 & 0 & A_{66} & 0 & 0 & B_{66} & 0 & 0\\ B_{11} & B_{12} & 0 & D_{11} & D_{12} & 0 & 0 & 0\\ B_{12} & B_{22} & 0 & D_{12} & D_{22} & 0 & 0 & 0\\ 0 & 0 & B_{66} & 0 & 0 & D_{66} & 0 & 0\\ 0 & 0 & 0 & 0 & 0 & 0 & A_{44} & 0\\ 0 & 0 & 0 & 0 & 0 & 0 & 0 & A_{55}\end{bmatrix}\begin{bmatrix}\varepsilon_x\\ \varepsilon_\theta\\ \varepsilon_{x\theta}\\ k_x\\ k_\theta\\ k_{x\theta}\\ \varepsilon_{\theta z}\\ \varepsilon_{xz}\end{bmatrix}-\begin{bmatrix}N_X^T\\ N_\theta^T\\ 0\\ M_X^T\\ M_\theta^T\\ 0\\ 0\\ 0\end{bmatrix} \tag{10}$$

In this relation, the coefficients, D_{ij}, B_{ij} and A_{ij} are as follows:

$$\begin{bmatrix}A_{ij} & B_{ij} & D_{ij}\end{bmatrix}=\sum_{k=1}^{N}\int_{z_{k-1}}^{z_k}\bar{Q}_{ij}\left\{1,z,z^2\right\}dz \tag{11}$$

The forces and moments created by thermal loading are calculated by the following relationships:

$$\begin{bmatrix}N_x^T\\ N_\theta^T\end{bmatrix}=\sum_{k=1}^{N}\int_{z_{k-1}}^{z_k}\begin{bmatrix}Q_{11} & Q_{12}\\ Q_{12} & Q_{22}\end{bmatrix}\begin{bmatrix}\alpha_{11}\\ \alpha_{22}\end{bmatrix}\Delta T dz \tag{12}$$

$$\begin{bmatrix}M_x^T\\ M_\theta^T\end{bmatrix}=\sum_{k=1}^{N}\int_{z_{k-1}}^{z_k}\begin{bmatrix}Q_{11} & Q_{12}\\ Q_{12} & Q_{22}\end{bmatrix}\begin{bmatrix}\alpha_{11}\\ \alpha_{22}\end{bmatrix}\Delta T z dz \tag{13}$$

with regard to the loading symmetry and the geometry of the problem relative to the cylinder axis, the strain components can be considered as follows [31]:

$$N_X=A_{11}\varepsilon_x+A_{12}\varepsilon_\theta+B_{11}k_x-N_x^T \tag{14}$$

$$N_\theta=A_{12}\varepsilon_x+A_{22}\varepsilon_\theta+B_{12}k_x-N_\theta^T \tag{15}$$

$$M_X = B_{11}\varepsilon_x + B_{12}\varepsilon_\theta + D_{11}k_x - M_x^T \tag{16}$$

$$M_\theta = B_{12}\varepsilon_x + B_{22}\varepsilon_\theta + D_{12}k_x - M_\theta^T \tag{17}$$

$$Q_x = A_{55}\varepsilon_{xz} \tag{18}$$

To obtain the equations of motion, we use Hamilton's principle for these equations. The general form of this principle is as follows [32]:

$$\int_0^T \delta L dt = \int_0^T (\delta K - \delta U) dt = 0 \tag{19}$$

After performing several integral integrators and separating the coefficients for δu, δv, δw, the motion equations are as follows [33, 34]:

$$N_{x,x} + \frac{N_{\theta x,\theta}}{R} = I_1 \ddot{u}_0 + I_2 \ddot{\psi}_x \tag{20}$$

$$\frac{N_{\theta,\theta}}{R} + N_{x\theta,x} + \frac{Q_\theta}{R} = I_1 \ddot{v}_0 + I_2 \psi_\theta \tag{21}$$

$$-\frac{N_\theta}{R} + Q_{x,x} + \frac{Q_{\theta,\theta}}{R} - Rq_z = I_1 \ddot{w}_0 + I_2 \psi_z + \frac{I_3}{2}\ddot{\phi}_z \tag{22}$$

$$M_{x,x} + \frac{M_{\theta x,\theta}}{R} - Q_x = I_2 \ddot{u}_0 + I_3 \ddot{\psi}_x \tag{23}$$

$$M_{x\theta,x} + \frac{M_{\theta,\theta}}{R} - Q_\theta = I_2 \ddot{v}_0 + I_3 \ddot{\psi}_\theta \tag{24}$$

Due to the axial symmetry of geometry and loading, ($\partial/\partial\theta = 0$), the number of motion equations for dynamic cylindrical shell behavior is reduced in the general case of sanders theory and Eqs. (2) and (5) are self-sufficient [35]. The motion equations in this case will be as follows:

$$A_{11}\frac{\partial^2 u}{\partial x^2} + \frac{A_{12}}{R}\frac{\partial w}{\partial x} + B_{11}\frac{\partial^2 \psi_x}{\partial x^2} - at_1^2\frac{\partial T_0}{\partial x} - bt_1^2\frac{\partial T_1}{\partial x} = I_1\frac{\partial^2 u}{\partial t^2} + \frac{1}{R}\frac{\partial^2 \psi_x}{\partial t^2} \tag{25}$$

$$A_{55}\frac{\partial^2 w}{\partial x^2} + A_{55}\frac{\partial \psi_x}{\partial x} - \frac{1}{R}\left(A_{12}\frac{\partial u}{\partial x} + A_{22}\frac{w}{R} + B_{12}\frac{\partial \psi_x}{\partial x} - \left(at_2^4 T_0 + bt_2^4 T_1\right)\right) = I_1\frac{\partial^2 w}{\partial t^2} \tag{26}$$

$$B_{11}\frac{\partial^2 u}{\partial x^2} + \frac{B_{12}}{R}\frac{\partial w}{\partial x} + D_{11}\frac{\partial^2 \psi_x}{\partial x^2} - bt_1^2\frac{\partial T_0}{\partial x} - ct_1^2\frac{\partial T_1}{\partial x} - A_{55}\frac{\partial w}{\partial x} - A_{55}\psi_x = \frac{I_2}{R}\frac{\partial^2 u}{\partial t^2} + I_3\frac{\partial^2 \psi_x}{\partial t^2} \tag{27}$$

To solve thermoelastic coupling problems, it is necessary to solve simultaneously the equations of motion and energy equations.

$$k_{ij}T_{ij} - \left[c_v \rho \dot{T} + T_a \beta_{ij}\dot{\varepsilon}_{ij}\right] = 0 \tag{28}$$

$$T\left(x,\theta,z,t\right)=T_0\left(x,\theta,t\right)+zT_1(x,\theta,t) \tag{29}$$

T_1 and T_0 are functions that we must obtain from the equation system. The Galerkin method is used to obtain two non-dependent thermal conductivity equations of Eq. (31). by averaging it in the thickness z of the shell, assuming a linear distribution in the thickness of the shell given by Eq. (32), the two variables T_1 and T_0 appear in the energy equations. For a multilayer cylindrical shell under thermal shock with axial symmetry and a uniform distribution along x, the energy Eq. (8) in terms of displacement terms is summarized as follows [36]:

$$Residual=\rho c\dot{T}+T_a\left[\beta_{xx}\dot{U}_{,x}+\frac{\beta_{\theta\theta}}{R+z}\dot{W}+\beta_{zz}\dot{W}_{,z}+\beta_{x\theta}\dot{V}_{,x}\right]-k_{xx}\frac{\partial^2T}{\partial x^2}-k_{zz}\left(\frac{\partial^2T}{\partial z^2}+\frac{1}{R+z}\frac{\partial T}{\partial z}\right) \tag{30}$$

The two integrals (32) and (33) yield two non-dependent energy equations, using two non-dependent T_1 and T_0 functions:

$$\int_z(Residual).(1).dz=0, \tag{31}$$

$$\begin{aligned}&R_c^{(1)}\dot{T}_0+R_c^{(2)}\dot{T}_1+R_x^{(1)}\dot{u}_{0,x}+R_x^{(2)}\dot{\psi}_{x,x}+R_{\theta x}^{(1)}\dot{\psi}_{\theta,x}+R_{\theta x}^{(1)}\dot{v}_{0,x}+R_z^{(2)}\dot{\psi}_z+R_x^{(2)}\dot{\varphi}_z+\frac{1}{R}R_\theta^{(1)}\dot{w}_0+\frac{1}{R}R_\theta^{(2)}\dot{\psi}_z\\&+\frac{1}{2R}R_\theta^{(3)}\dot{\varphi}_z+R_{kx}^{(1)}\dot{T}_{0,xx}+R_{kx}^{(2)}\dot{T}_{1,xx}-\frac{1}{R}R_{kz}^{(1)}T_1-\left(h_i-h_o\right)T_0+h\left(h_i-h_o\right)T_1+\left[h_iT_i\left(t\right)-h_0T_\infty\right]=0\end{aligned} \tag{32}$$

and

$$\int_z(Residual).(z).dz=0, \tag{33}$$

$$\begin{aligned}&R_c^{(2)}\dot{T}_0+R_c^{(3)}\dot{T}_1+R_x^{(2)}\dot{u}_{0,x}+R_x^{(3)}\dot{\psi}_{x,x}+R_{\theta x}^{(2)}\dot{\psi}_{\theta,x}+R_{\theta x}^{(2)}\dot{v}_{0,x}+R_z^{(3)}\dot{\psi}_z+R_x^{(3)}\dot{\varphi}_z+\frac{1}{R}R_\theta^{(2)}\dot{w}_0+\frac{1}{R}R_\theta^{(3)}\dot{\psi}_z\\&+\frac{1}{2R}R_\theta^{(4)}\dot{\varphi}_z+R_{kx}^{(2)}\dot{T}_{0,xx}+R_{kx}^{(3)}\dot{T}_{1,xx}-\frac{1}{R}R_{kz}^{(2)}T_1-h[\left(h_i-h_o\right)T_0-\left(h_i-h_o\right)T_1-(h_iT_i\left(t\right)-h_0T_\infty)]=0\end{aligned} \tag{34}$$

In these equations, some of the parameters are eliminated due to the axial symmetry ($\partial/\partial\theta=0$). Relationships for the coefficients $R_j^{(K)}$ are given in the appendix.

As already mentioned, β is the volumetric expansion coefficient and k is the conduction coefficients in different directions of the composite. To solve the problem, we need to solve a device that contains the equations of motion and energy equations. These equations are in the partial derivative (pde), that is, the function x and t. To solve the equations, we need to write them to the finite element matrix form $M\ddot{x}+C\dot{x}+Kx=F$. Matrix form can be used in a variety of ways, including the Rang Kuta method. The steps in converting the pde equations into the matrix form of the finite element are as follows. First, using the Galerkin method, we write the equations in a weak form, and then write them in a common matrix.

The initial conditions of the problem are considered zero:

$$u_0\left(x,0\right)=w_0\left(x,0\right)=\psi_{x0}\left(x,0\right)=0 \tag{35}$$

$$\frac{\partial u_0\left(x,0\right)}{\partial t}=\frac{\partial w_0\left(x,0\right)}{\partial t}=\frac{\partial\psi_{x0}\left(x,0\right)}{\partial t}=0 \tag{36}$$

The weak form of the equations will be:

$$-A_{11}\int_0^L\left(\frac{\partial u}{\partial x}\frac{\partial w_1}{\partial x}\right)dx+\frac{A_{12}}{R}\int_0^L(\frac{\partial w}{\partial x}w_1)dx-B_{11}\int_0^L\left(\frac{\partial \psi_x}{\partial x}\frac{\partial w_1}{\partial x}\right)dx-at_1^2\int_0^L\left(\frac{\partial T_0}{\partial x}\right)w_1dx-bt_1^2\int_0^L\left(\frac{\partial T_1}{\partial x}\right)w_1$$
$$-I_1\int_0^L\frac{\partial^2 u}{\partial t^2}w_1dx-I_2\int_0^L\frac{\partial^2\psi_x}{\partial t^2}w_1dx=0 \tag{37}$$

$$-A_{55}\int_0^L\left(\frac{\partial w}{\partial x}\frac{\partial w_2}{\partial x}\right)dx+A_{55}\int_0^L(\frac{\partial \psi_x}{\partial x}w_2)dx-\frac{A_{12}}{R}\int_0^L(\frac{\partial u}{\partial x}w_2)dx-\frac{A_{22}}{R^2}\int_0^L ww_2dx-\frac{B_{12}}{R}\int_0^L(\frac{\partial\psi_x}{\partial x}w_2)dx$$
$$+\frac{at_2^4}{R}\int_0^L T_0w_2-\frac{bt_2^4}{R}\int_0^L T_1w_2-I_1\int_0^L\frac{\partial^2 w}{\partial t^2}w_2dx=0 \tag{38}$$

$$-B_{11}\int_0^L\left(\frac{\partial u}{\partial x}\frac{\partial w_3}{\partial x}\right)dx+\frac{B_{12}}{R}\int_0^L(\frac{\partial w}{\partial x}w_3)dx-D_{11}\int_0^L\left(\frac{\partial\psi_x}{\partial x}\frac{\partial w_3}{\partial x}\right)dx-A_{55}\int_0^L(\frac{\partial w}{\partial x}w_3)dx-A_{55}\int_0^L\psi_xw_3dx-bt_1^2\int_0^L\left(\frac{\partial T_0}{\partial x}\right)w_3dx$$
$$-ct_1^2\int_0^L\left(\frac{\partial T_1}{\partial x}\right)w_3-I_2\int_0^L\frac{\partial^2 u}{\partial t^2}w_3dx-I_3\int_0^L\frac{\partial^2\psi_x}{\partial t^2}w_3dx=0 \tag{39}$$

$$\frac{R_c^{(1)}L}{2}\dot{T_0}+\frac{R_c^{(2)}L}{2}\dot{T_1}+\frac{R_x^{(1)}(m\pi)}{2}\dot{u}+\frac{R_x^{(2)}(m\pi)}{2}\dot{\psi}_x+\frac{R_\theta^{(1)}L}{2R}\dot{w}_0-\frac{R_{kx}^{(1)}(m\pi)^2}{2L}T_0-\frac{R_{kx}^{(2)}(m\pi)^2}{2L}T_1$$
$$+\frac{R_{kz}^{(1)}L}{2R}T_1-\frac{(h_i-h_o)L}{2}T_0+\frac{(h_i-h_o)hL}{2}T_1-[h_iT_i(t)-h_0T_\infty]\frac{L}{m\pi}cos(\frac{m\pi}{L}x)]_0^L=0 \tag{40}$$

$$\frac{R_c^{(2)}L}{2}\dot{T_0}+\frac{R_c^{(3)}L}{2}\dot{T_1}+\frac{R_x^{(2)}(m\pi)}{2}\dot{u}+\frac{R_x^{(3)}(m\pi)}{2}\dot{\psi}_x+\frac{R_\theta^{(2)}L}{2R}\dot{w}_0-\frac{R_{kx}^{(2)}(m\pi)^2}{2L}T_0-\frac{R_{kx}^{(3)}(m\pi)^2}{2L}T_1$$
$$+\frac{R_{kz}^{(2)}L}{2R}T_1-\frac{h(h_i-h_o)L}{2}T_0+\frac{(h_i-h_o)hL}{2}T_1+[h_iT_i(t)-h_0T_\infty]\frac{L}{m\pi}cos(\frac{m\pi}{L}x)]_0^L=0 \tag{41}$$

By integrating the final form of the ode's equations is as follows:

$$-\frac{A_{11}(m\pi)^2}{2L}U_m+\frac{A_{12}(m\pi)}{2R}W_m-\frac{B_{11}(m\pi)^2}{2L}\psi_x-at_1^2\frac{(m\pi)}{2}T_{0m}-bt_1^2\frac{(m\pi)}{2}T_{1m}-\frac{LI_1}{2}\ddot{U}_m(t)$$
$$-\frac{LI_2}{2}\ddot{\psi}_{xm}(t)=0 \tag{42}$$

$$-\frac{RA_{12}(m\pi)}{2}U_m+\frac{A_{22}L}{2}W_m-\frac{RA_{55}(m\pi)}{2}\psi_{xm}-\frac{Rat_2^4L}{2}T_{0m}-\frac{Rbt_2^4L}{2}T_{1m}-\frac{A_{55}(m\pi)^2}{2L}W_m$$
$$-\frac{I_1L}{2}\ddot{W}=0 \tag{43}$$

$$-\frac{B_{11}(m\pi)^2}{2L}U_m-\frac{D_{11}(m\pi)^2}{2L}\psi_{xm}-\frac{A_{55}(m\pi)}{2R}W_m-\frac{a_{45}L}{2}\psi_{xm}-\frac{LI_2}{2}\ddot{U}_m-\frac{LI_3}{2}\ddot{\psi}_m-\frac{bt_1^2(m\pi)}{2}T_{0m}$$
$$-\frac{ct_1^2(m\pi)}{2}T_{1m}=0 \tag{44}$$

$$\frac{R_c^{(1)}L}{2}\dot{T_0}+\frac{R_c^{(2)}L}{2}\dot{T_1}+\frac{R_x^{(1)}(m\pi)}{2}\dot{u}+\frac{R_x^{(2)}(m\pi)}{2}\dot{\psi}_x+\frac{R_\blacklozenge^{(1)}L}{2R}\dot{w}_0-\frac{R_{kx}^{(1)}(m\pi)^2}{2L}T_0-\frac{R_{kx}^{(2)}(m\pi)^2}{2L}T_1$$
$$+\frac{R_{kz}^{(1)}L}{2R}T_1-\frac{(h_i-h_o)L}{2}T_0+\frac{(h_i-h_o)hL}{2}T_1-[h_iT_i(t)-h_0T_\infty]\frac{L}{m\pi}cos(\frac{m\pi}{L}x)]_0^L=0 \tag{45}$$

$$\frac{R_c^{(2)}L}{2}\dot{T}_0+\frac{R_c^{(3)}L}{2}\dot{T}_1+\frac{R_x^{(2)}(m\pi)}{2}\dot{u}+\frac{R_x^{(3)}(m\pi)}{2}\dot{\psi}_x+\frac{R_\theta^{(2)}L}{2R}\dot{w}_0-\frac{R_{kx}^{(2)}(m\pi)^2}{2L}T_0-\frac{R_{kx}^{(3)}(m\pi)^2}{2L}T_1$$
$$+\frac{R_{kz}^{(2)}L}{2R}T_1-\frac{h(h_i-h_o)L}{2}T_0+\frac{(h_i-h_o)hL}{2}T_1+[h_iT_i(t)-h_0T_\infty]\frac{L}{m\pi}cos(\frac{m\pi}{L}x)]_0^L=0 \quad (46)$$

Now, the equations can be written in the form of the matrix $M\ddot{x}+C\dot{x}+Kx=F$, and this equation can be solved by different methods. In this study, the Runge–Kutta methods has been used.

3 RUNGE-KUTTA FOURTH-ORDER METHOD

This method was first presented by two German mathematicians named Renge and Kuta. This method has several levels that we use in this paper from its fourth order state. Runge-Kutta fourth order method is a numerical technique used to solve ordinary differential equation of the form

$$\frac{dy}{dx}=f(x,y),y(0)=y_0 \quad (47)$$

K_1, K_2, K_3, and K_4 are the values of the Rang Kuta method, which should be weighted average of these values with the values of displacement and velocity in the previous step in order to calculate the velocity and displacement in each step [37].

$$k_1=hf(x_i,y_i),\quad k_2=hf\left(x_i+\frac{h}{2},y_i+\frac{k_1}{2}\right),\ k_3=hf\left(x_i+\frac{h}{2},y_i+\frac{k_2}{2}\right),\ k_4=hf(x_i+h,y_i+k_3)$$
$$y_{i+1}=y_i+\frac{1}{6}(k_1+2k_2+2k_3+k_4) \quad (48)$$

which h is time step of solving.

4 NUMERICAL RESULTS AND DISCUSSION

In this section of the work, we will verify the results of the research with other studies of scholars that are presented in valid journals. For this purpose, we compared the results of the radial motion of the intermediate layer with the results of the Jeng-Shian Chang et al [28], which can be seen in the Figs. 2-4 for the shells of different fiber angles. In all of these cases, the shell is considered as a double-headed. As you can see, the results are very close to the results of Chang et al [28] work.

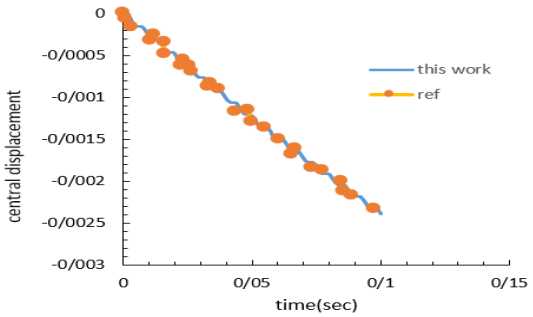

Fig.2
Comparison of the interlayer displacement for the fiber angle (45,- 45, 45, -45) with ref [6].

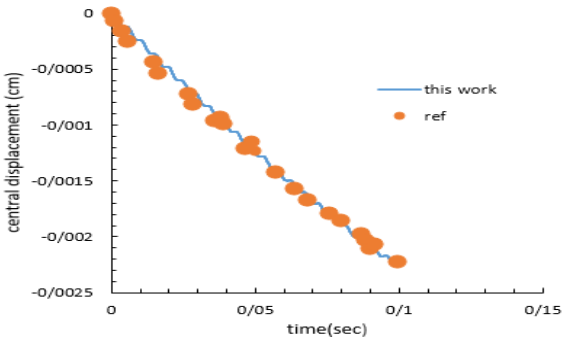

Fig.3
Comparison of the interlayer displacement for the fiber angle (0, 90, 0, 90) with ref [6].

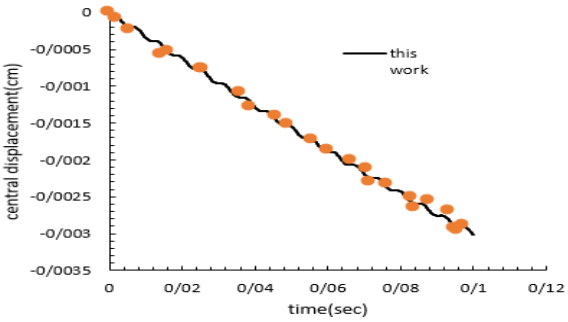

Fig.4
Comparison of the interlayer displacement for the fiber angle (0, 0, 0, 0) with ref [6].

All results are obtained using the properties listed in the Table 1. Otherwise, the values that have been changed in the description of the image are listed.

Table 1
Geometry and material properties of composite shell.

Parameter value	Parameter
25.4 *cm*	Cylindrical length (L)
50 *cm*	Middle layer radius (R)
0.0635*cm*	Thickness of each layer (H)
(-45,45,-45,45)	Fiber angle
137.9 *Gpa*	Young's modulus for direction 1 (E_{11})
8.96 *Gpa*	Young's modulus for direction 2 and 3 (E_{22}=E_{33})
7.1 *Gpa*	Shear modulus (G_{12}=G_{13})
3.447 *Gpa*	Shear modulus (G_{23})
0.3	Poisson's ratio (υ)
46.2×10^{-3} *J/cm s K*	Heat transfer coefficient in direction 1 (K_{11})
7.2×10^{-3} *J/cm s K*	Heat transfer coefficient in direction 2 and 3 (K_{22}=K_{33})
16.35 J/cm^2 *s*	Thermal shock load (f_t)
100 ^oC	Initial temperature change ($\Delta\Theta$)

The effect of change in shell thickness on the displacement of the middle layer and frequency is shown in Figs. 5 and 6.

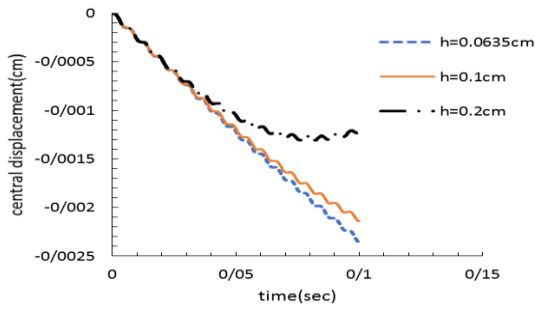

Fig.5
Changes in the radial displacement of the interlayer in different thicknesses of the layers.

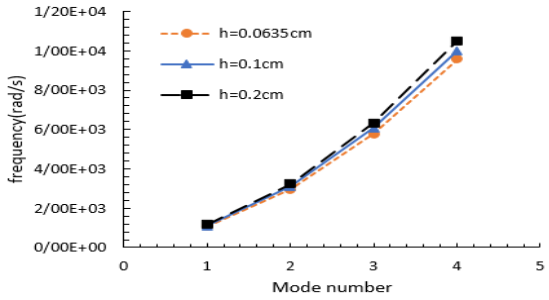

Fig.6
Changes in natural frequencies by changing the thickness of the layers.

In Figs. 7 and 8, the length of the cylindrical length parameter is investigated. It is seen that in Fig. 7, with increasing length of the cylinder, the displacement of the middle layer is increased, as can be seen in Fig. 8, by increasing the length of the cylinder. The natural frequency has decreased.

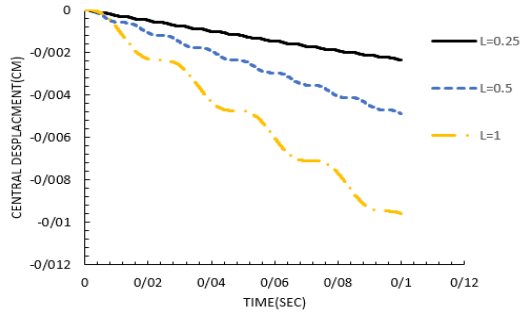

Fig.7
Change in the radial displacement of the middle layer by changing the length of the cylinder.

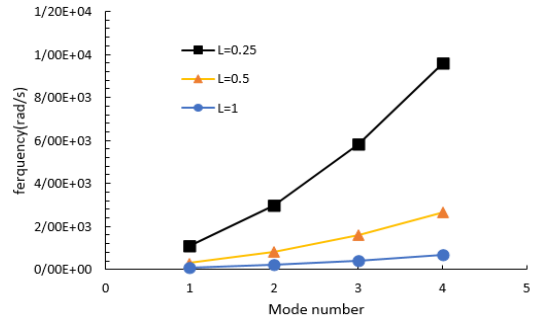

Fig.8
Change in natural frequencies by changing the length of the cylinder.

Another important geometric parameter in the cylindrical shell is the radius of the intermediate layer, which in Figs. 9 and 10, respectively, deals with the effects of the middle layer radius on the displacement of the middle layer and the frequency. By increasing the radius, the displacement Dropped. In Fig. 10, it is also observed that the natural frequency increased by increasing the radius.

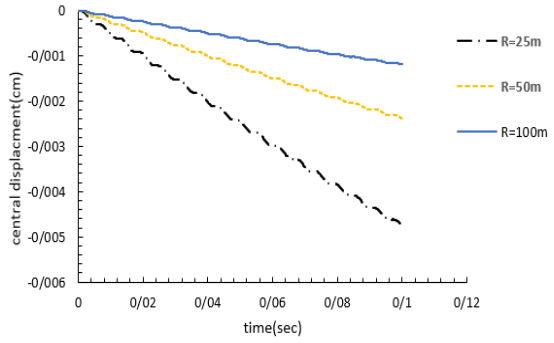

Fig.9
Changes in the radial displacement of the intermediate layer by changing the radius of the cylinder.

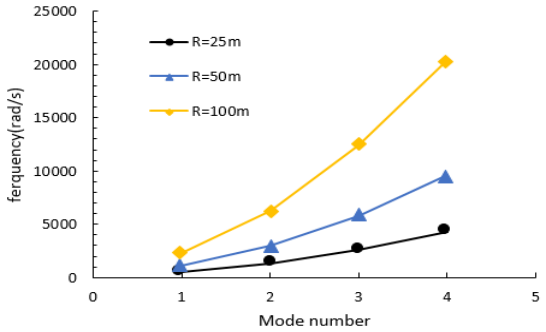

Fig.10
Change in natural frequencies by changing the radius of the cylinder.

In the next study, Fig.11 shows the effect of different angles of the fiber in the dynamic response.

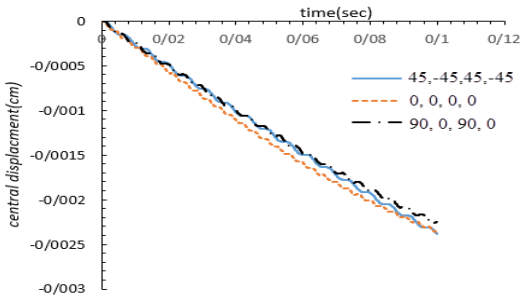

Fig.11
Changes in the radial displacement of the intermediate layer by changing the Fiber angle.

The basic parameter to be considered in this study is the effect of the shock load (f_i) on the range of vibration displacement. The result of this study is shown in Fig. 12.

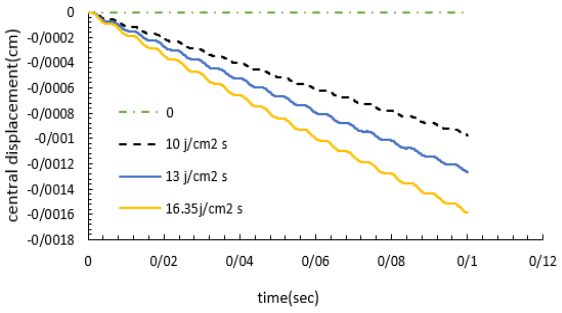

Fig.12
Changes in the radial displacement of the intermediate layer with a change in thermal shock.

Figs. 13 and 14 show a change in the natural frequency and displacement of the middle layer by changing the thermal field temperature. As the temperature rises, the material becomes softer so that the displacement rises, but due to the initial stresses it causes that the natural frequency decreases. Fig. 13 shows that the field does not have much effect on the original frequency (first frequency), but the increase of the field affects the subsequent frequencies and reduces the frequency.

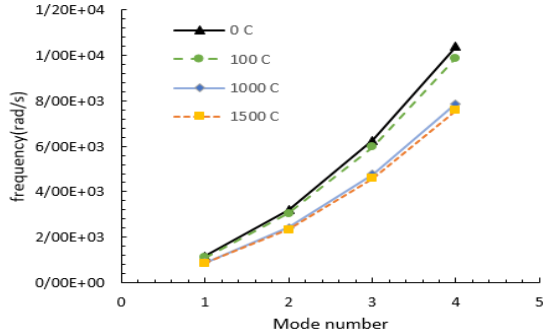

Fig.13
Changes in natural frequencies by changing the temperature of the initial thermal field.

In Fig. 14 it is seen that the existence of a mild initial field (up to 100 degrees) does not have much effect on the dynamic response but will reduce the natural shell frequencies (especially higher frequencies). However, the thermal field does not have a significant effect on the dynamic response in the short time, but after a while it reduces the hardness matrix values and will reduce the frequency and increase the range of displacement.

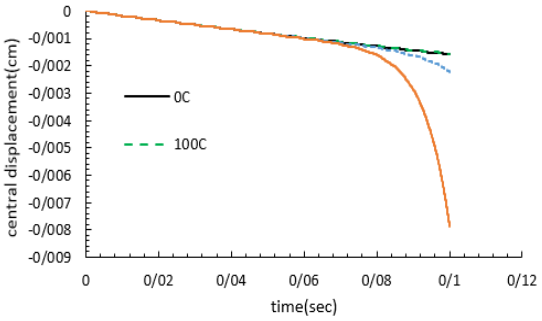

Fig.14
Changes in the radial displacement of the intermediate layer with a change in Thermal field.

5 CONCLUSION

In this paper, the dynamics and vibrational responses of cylindrical shells of thin-walled composite materials under the primary thermal field and thermal shock were investigated. The influence of parameters such as radius, cylindrical length, shell thickness, temperature of the field and ... on the range of radial displacement of the middle layer and Natural frequencies were dealt with. By examining the effects of the heat field and thermal shock, it was found that a mild heat field (far away from the melting point of the composite matrix) does not have an effect on the dynamic response but reduces the natural frequency, especially higher frequencies. But the effect of increasing the thermal shock on the increase in displacement is considerable, but with transient effects it has no effect on natural frequencies.

APPENDIX

$$R_{kz}^{(1)} = \sum_{i=1}^{N} k_{zz}^{i} (h_i - h_{i-1}),$$

$$R_{kz}^{(2)} = \sum_{i=1}^{N} \int_{h_{j-1}}^{h_j} k_{zz}^{j} z dz ,$$

$$R_{kx}^{(i)} = \sum_{i=1}^{N} \int_{h_{j-1}}^{h_j} k_{xx}^{j} z^{(i-1)} dz \quad i = 1,2,3$$

$$R_{c}^{(i)} = \sum_{i=1}^{N} \int_{h_{j-1}}^{h_j} < \rho c_v >_j z^{(i-1)} dz \quad i = 1,2,3$$

$$R_{x}^{(i)} = \sum_{i=1}^{N} \int_{h_{j-1}}^{h_j} < T_a \beta_{xx} >_j z^{(i-1)} dz \quad i = 1,2,3$$

$$R_{\theta}^{(i)} = \sum_{i=1}^{N} \int_{h_{j-1}}^{h_j} < T_a \beta_{\theta\theta} >_j z^{(i-1)} dz \quad i = 1,2,3$$

$$R_{z}^{(i)} = \sum_{i=1}^{N} \int_{h_{j-1}}^{h_j} < T_a \beta_{zz} >_j z^{(i-1)} dz \quad i = 1,2,3$$

$$R_{x\theta}^{(i)} = \sum_{i=1}^{N} \int_{h_{j-1}}^{h_j} < T_a \beta_{x\theta} >_j z^{(i-1)} dz \quad i = 1,2,3$$

REFERENCES

[1] McQuillen E.J., Brull M.A., 1970, Dynamic thermoelastic response of cylindrical shells, *Journal of Applied Mechanics* **37**(3): 661-670.

[2] Biot M.A., 1956, Thermoelasticity and irreversible thermodynamics, *Journal of Applied Physics* **27**(3): 240-253.

[3] Timoshenko S., Winoowsky-Krieger S., 1959, *Theory of Plates and Shells*, McGraw-Hill.

[4] Boley B.A., Weiner J.H., 1960, *Theory of Thermal Stresses*, John Wiley & Sons.

[5] Nowacki W., 1962, *Thermoelasticity*, Pergamon Press.

[6] Ugural A.C., 1981, *Stresses in Plates and Shells*, McGraw-Hill.

[7] Awrejcewicz J., Krysko V.A., 2003, Coupled thermoelasticity problems of shallow shells, *Systems Analysis Modelling Simulation* **43**(3): 269-286.

[8] Awrejcewicz J., Krysko V.A., 2003, Nonlinear coupled problems in dynamics of shells, *International Journal of Engineering Science* **41**(6): 587-607.

[9] Huth J.H., 1953, Thermal stress in conical shells, *Aeronaut* **20**: 613-616.

[10] Huth J.H., 1955, Thermal stress in conical shells, *Aeronaut* **22**: 506-508.

[11] Eslami M.R., Vahedi H., 1991, A general finite element stress formulation of dynamic thermoelastic problems using Galerkin method, *Journal of Thermal Stresses* **14**: 143-159.

[12] Eslami M.R., Shakeri M., Sedaghati R., 1994, Coupled thermoelasticity of axially symmetric cylindrical shell, *Journal of Thermal Stresses* **17**(1): 115-135.

[13] Eslami M.R., Shakeri M., Ohadi A.R., Shiari B., 1999, Coupled thermoelasticity of shells, effect of normal stress and coupling, *AIAA Journal* **37**(4): 496-504.

[14] Hakimelahi B., Soltani N., 1999, A solution for the coupled dynamic thermoelastic problems of thin cylindrical shells under pressure shear and temperature shocks using finite element methods, *Journal of Faculty of Engineering* **33**(3): 73-86.

[15] Eslami M. R., Mousavi S. M., 1998, Dynamic analysis of conical shells under mechanical and thermal loading by Galerkin finite element method, *Second Conference of Aerospace Engineering*, Iran.

[16] Tarn J.Q., 2001, Exact solutions for functionally graded anisotropic cylinders subjected to thermal and mechanical loads, *International Journal of Solids and Structures* **38**(46-47): 8189-8206.

[17] Alibeigloo A., 2011, Thermoelastic solution for static deformations of functionally graded cylindrical shell bonded to thin piezoelectric layers, *Composite Structures* **93**(2): 961-972.

[18] Ansari R., Torabi J., Faghih Shojaei M., 2016, Free vibration analysis of embedded functionally graded carbon nanotube-reinforced composite conical/cylindrical shells and annular plates using a numerical approach, *Journal of Vibration and Control* **24**(6): 1123-1144.

[19] Alibeigloo A., 2016, Elasticity solution of functionally graded carbon nanotube-reinforced composite cylindrical panel subjected to thermo mechanical load, *Composites Part B: Engineering* **87**: 214-226.

[20] Kiani Y., Eslami M.R., 2014, Geometrically non-linear rapid heating of temperature-dependent circular FGM plates, *Journal of Thermal Stresses* **37**(12): 1495-1518.

[21] Ghiasian S.E., Kiani Y., Eslami M.R., 2014, Non-linear rapid heating of FGM beams, *International Journal of Non-Linear Mechanics* **67**: 74-84.

[22] Alipour S.M., Kiani Y., Eslami M.R., 2016, Rapid heating of FGM rectangular plates, *Acta Mechanica* **227**(2): 421-436.

[23] Keibolahi A., Kiani Y., Eslami M.R., 2018, Nonlinear rapid heating of shallow arches, *Journal of Thermal Stresses* **41**(10-12): 1244-1258.

[24] Esmaeili H.R., Arvin H., Kiani Y., 2019, Axisymmetric nonlinear rapid heating of FGM cylindrical shells, *Journal of Thermal Stresses* **42**(4): 490-505.

[25] Keibolahi A., Kiani Y., Eslami M.R., 2018, Dynamic snap-through of shallow arches under thermal shock, *Aerospace Science and Technology* **77**: 545-554.

[26] Javani M., Kiani Y., Eslami M.R., 2019, Geometrically nonlinear rapid surface heating of temperature-dependent FGM arches, *Aerospace Science and Technology* **90**: 264-274.

[27] Javani M., Kiani Y., Eslami M.R., 2019, Large amplitude thermally induced vibrations of temperature dependent annular FGM plates, *Composites Part B: Engineering* **163**: 371-383.

[28] Chang J.S., Shyong J.W., 1994, Thermally induced vibration of laminated circular cylindrical shell panels, *Composites Science and Technology* **51**(3): 419-427.

[29] Bert C.W., Kumar M., 1982, Vibration of cylindrical shells of bimodulus composite materials, *Journal of Sound and Vibration* **81**(1):107-121.

[30] Vinson J.R., Sierakowski R.L., 2006, *The Behavior of Structures Composed of Composite Materials*, Springer Science & Business Media.

[31] Eslami M.R., Shakeri M., Sedaghati R., 1994, Coupled thermoelasticity of an axially symmetric cylindrical shell, *Journal of Thermal Stresses* **17**(1): 115-135.

[32] Pothula S.G., 2009, *Dynamic Response of Composite Cylindrical Shells under External Impulsive Loads*, PhD Thesis, University of Akron.

[33] Kang S.G., Young K.J., 2016, Thermo-mechanical response of multi-layered cylinders under pressure and thermal loading with generalized plane strain condition, *ASME 2016 Pressure Vessels and Piping Conference*, American Society of Mechanical Engineers.

[34] Zhengwei H., Chengjun W., 2015, Vibration analysis for the cylindrical shell and plate composite structure using the mixed-mode substructure method, *Proceedings of the 22nd International Congress on Sound & Vibration*, Florence, Italy.

[35] Eslami M., Vahedi H., 1992, Galerkin finite element displacement formulation of coupled thermoelasticity spherical problems, *Journal of Pressure Vessel Technology* **114**(3): 380-384.

[36] Shiari B., Eslami M.R., Shaker M., 2003, Thermomechanical shocks in composite cylindrical shells: a coupled thermoelastic finite element analysis, *Scientia Iranica* **10**(1): 13-22.

[37] Prince P.J., Dormand J.R., 1981, High order embedded Runge-Kutta formulae, *Journal of Computational and Applied Mathematics* **7**(1): 67-75.